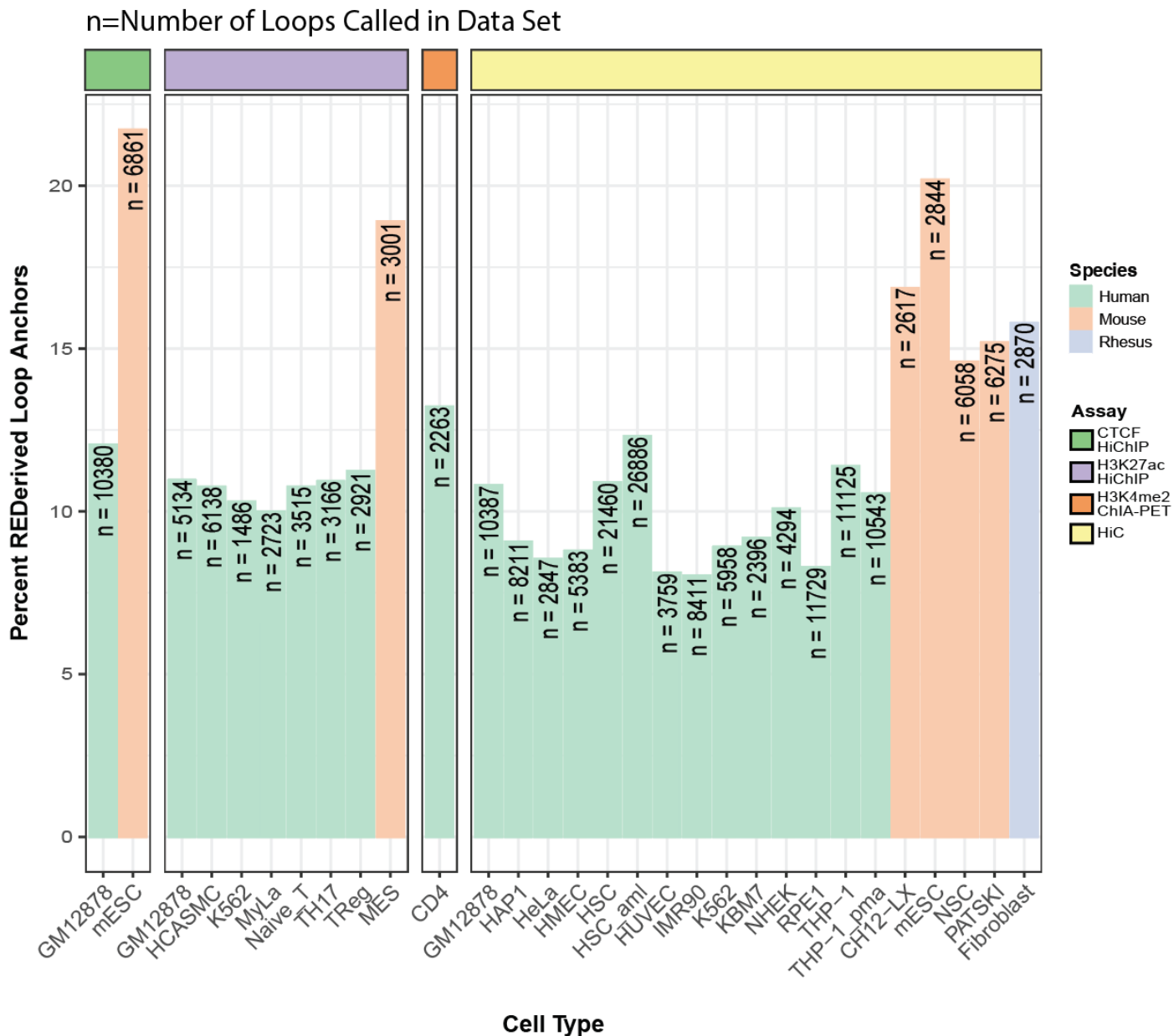


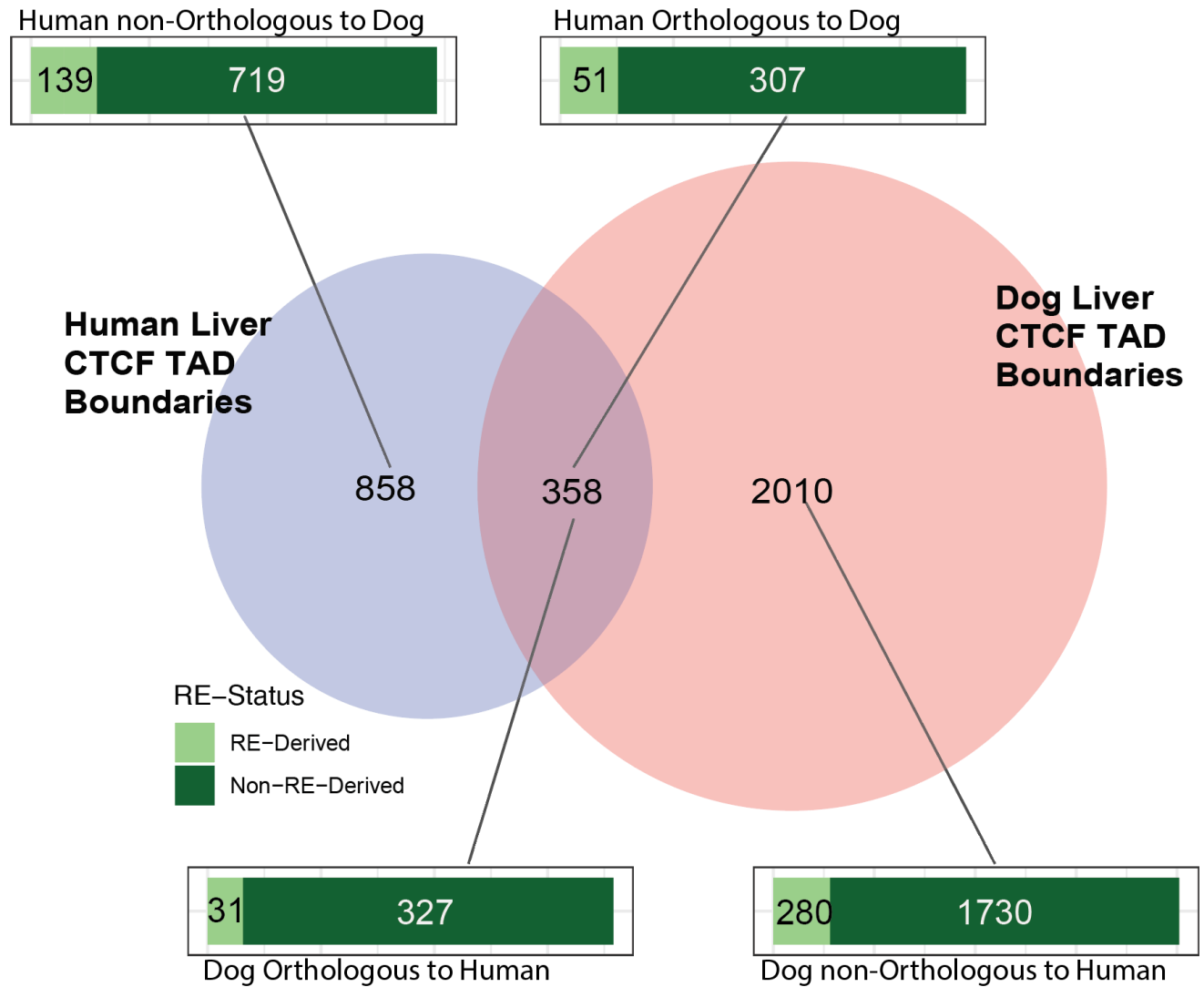
Supplementary Information

Supplementary Figure 1: Data Set Resolution compared with TE Contribution to Loop Anchors



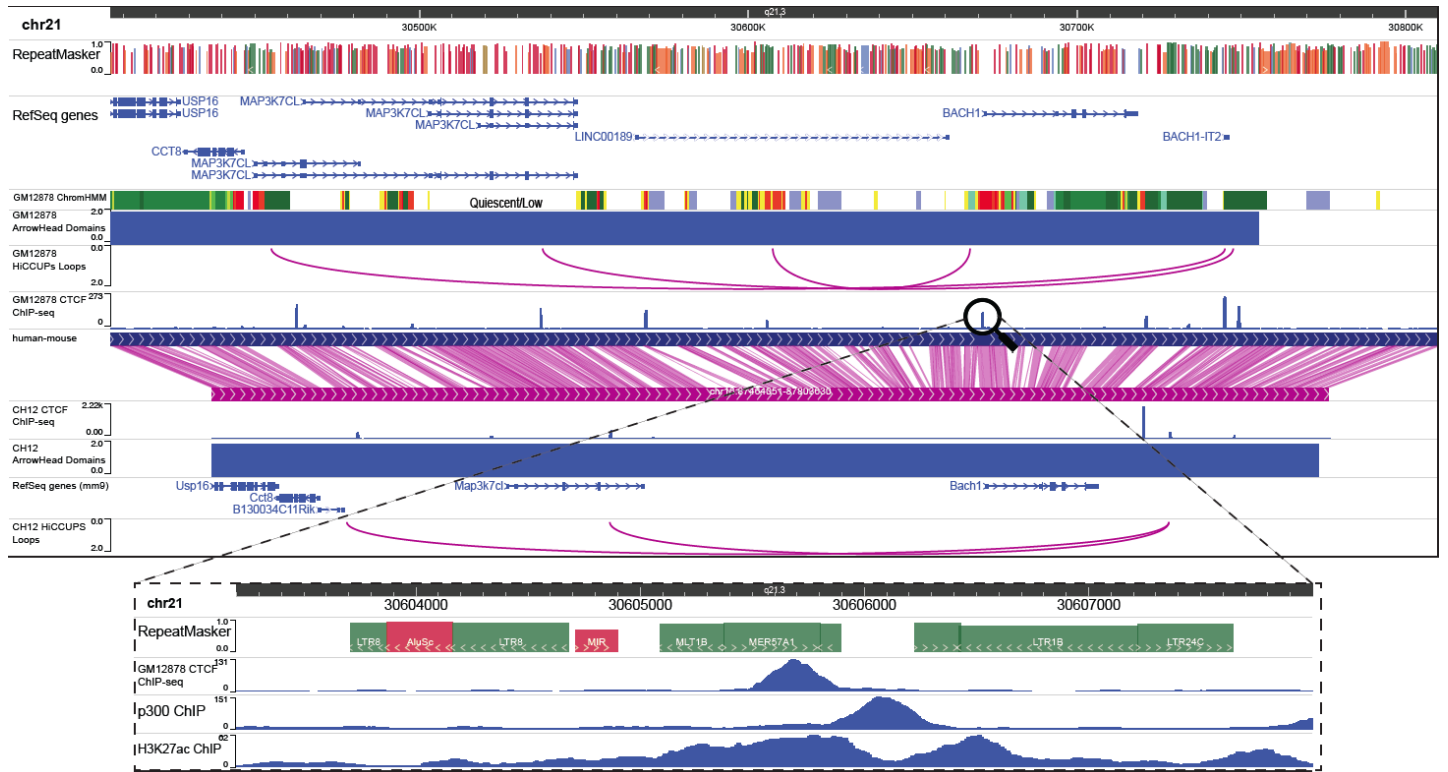
The number of loops called in each dataset is displayed in each of the corresponding bars. The y-axis shows the percent of loop anchors that overlap a repetitive element for each of the included datasets.

Supplementary Figure 3: Comparison of Human and Dog Liver CTCF TAD Boundaries



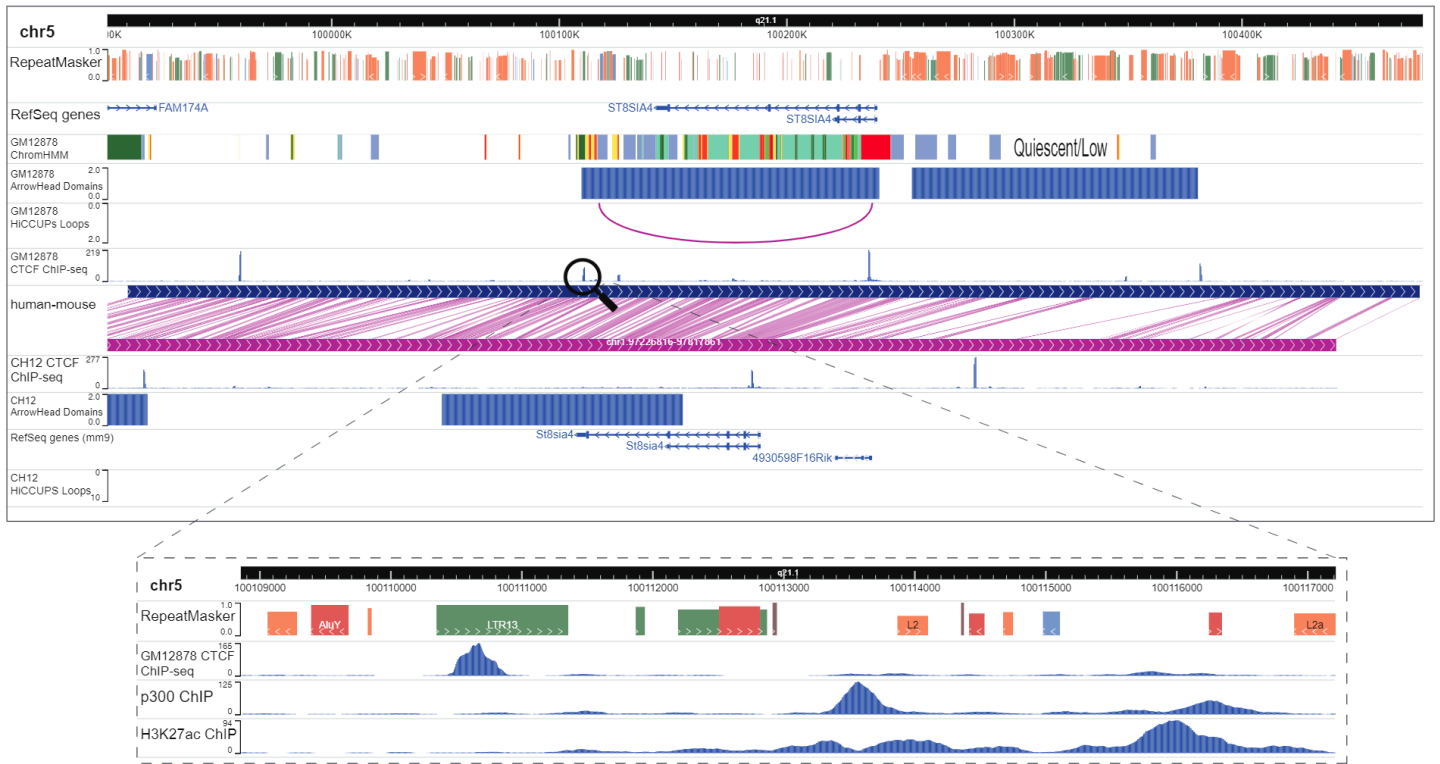
Dog liver TAD boundary data from Rudan et. al was lifted over from canFam3 to hg19 and compared with human liver data from Schmitt et. al to identify orthologous and non-orthologous CTCF TAD boundaries. The human liver data from Schmitt et. al was similarly lifted over to the canFam3 genome and compared to the dog liver data. These orthologous and non-orthologous TAD boundaries were then intersected with repeatMasker to identify RE-derived CTCF boundaries.

Supplementary Figure 4: MER57A1 Derived Loop Anchor



Genome browser screenshot displaying the MER57A1 candidate and the local histone, binding, 3D landscape in human (main top) and mouse (main bottom). Zoomed in view of the MER57A1 candidate with CTCF, p300, and H3K27ac ChIP-seq peaks (inset).

Supplementary Figure 5: LTR13 Derived Loop Anchor



Genome browser screenshot displaying the LTR13 candidate and the local histone, binding, 3D landscape in human (main top) and mouse (main bottom). Zoomed in view of the LTR13 candidate with CTCF, p300, and H3K27ac ChIP-seq peaks (inset).

Supplementary Figure 6: L1MC1-KO specific deletions:

Primers, L2 sgRNA, R1 sgRNA, R2 sgRNA, L1MC1, CTCF Motif

Genomic Sequence:

TTCACGCTTCACTTGTCTGCgtacctcattcttcttagacgcaggacaagagctctggcaaaggcgctgcagccacagaggttc
cggccggaaaaatcggcaccacagagatcccatgagaacgtcacgtacagcactgagacggagccctaataaaaactgtggctct
gggtgataatgacgttactgtgggttcatcaactgtagcaaatc**gcctctgctggg**cggtgttgaaatgcagagg**ctctggg**
gggtcaggtatgtgggagctctctgtacctttcttgaatttgatgtgaacttaagctgctccaaaaagataaaatcttgaaga
aaagcgaaaaaaaaaaggaagagagggaaaaaat**gacaggcagaaggtcacgcctgg**ccctcagtgcgctcctcaggcctc
tgctccagctggggctggcaggtggcggggggcaccagctcctccactccccacgcccaccacagctttcaaagttaggaa
cacaggcaggt**GGAGGTGAAGTCCGAACAGA**

Clone 1 (from forward primer):

TTCACGCTTCACTTGTCTGCgtacctcattcttcttagacgcaggacaagagctctggcaaaggcgctgcagccacagagg
tttccggccggaaaaatcggcaccacagagatcccatgagaacgtcacgtacagcactgagacggagccctaataaaaact
gtggctctg**gggtgataatgacgtta**.....
.....**tgt**gggagctctctgtacctttcttgaatttgatgtgaacttaagctgctccaaaa
gataaaatcttgaagaaaagcgaaaaaaaaaaggaagagagggaaaaaat**gacaggcagaaggtcacgcctgg**ccctc
agtgcgctcctcaggcctctgctccagctggggctggcaggtggcggggggcaccagctcctccactccccacgccc
caccacagctttcaaagttaggaaacagggcaggt**GGAGGTGAAGTCCGAACAGA**

Clone 47 (Heterozygous, double knockout)

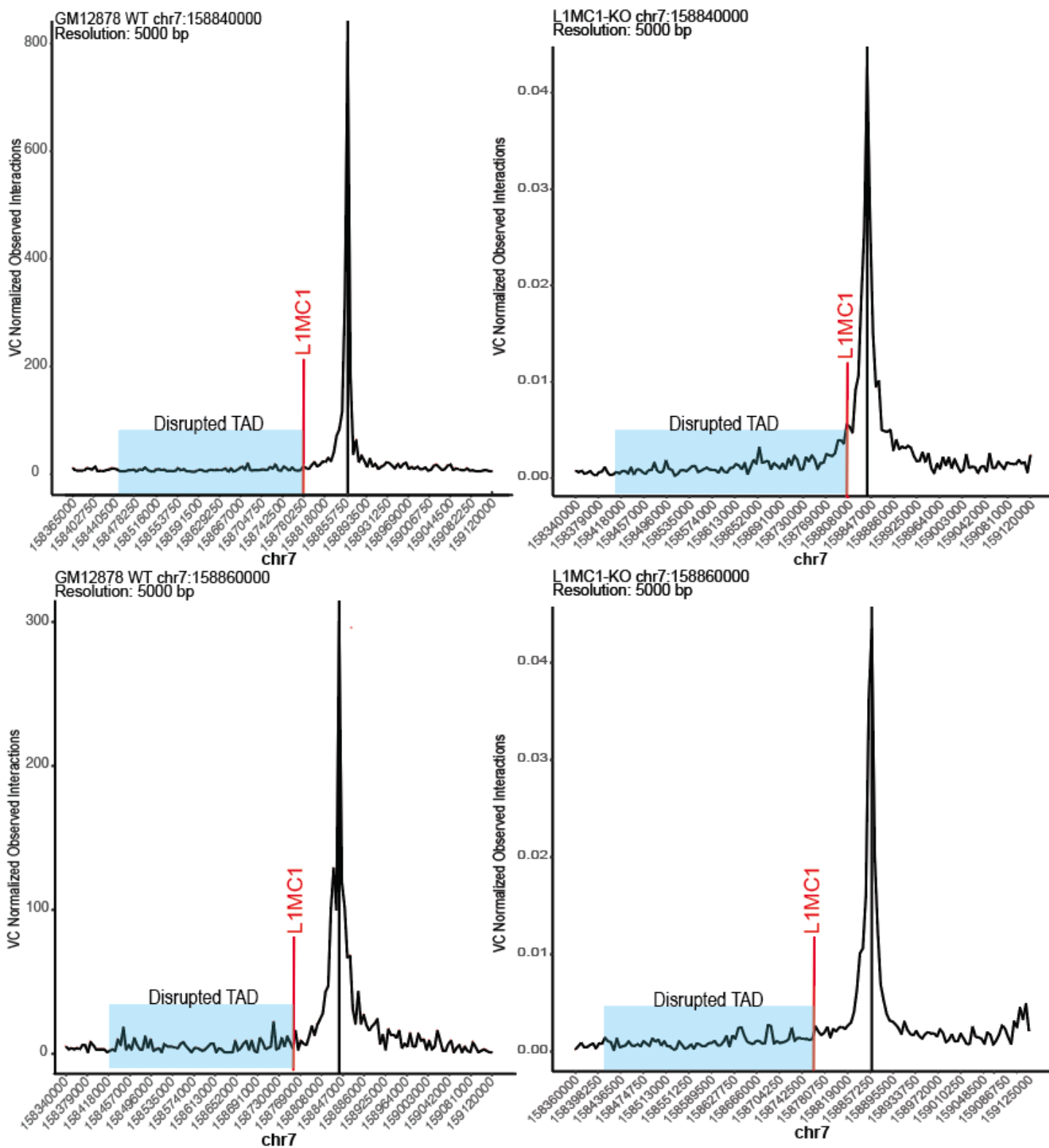
TTCACGCTTCACTTGTCTGCgtacctcattcttcttagacgcaggacaagagctctggcaaaggcgctgcagccacagagg
tttccggccggaaaaatcggcaccacagagatcccatgagaacgtcacgtacagcactgagacggagccctaataaaaact
gtggctct**gggtgataatgacgttactgtggg**ttcatcaactgtagcaaatc**gcctctgctggg**cggtgttgaaatgc
agaggctctggggggtcaggtatgtgggagctctctgtacctttcttgaatttgatgtgaacttaagctgctccaaaa
gataaaatcttgaagaaaagcgaaaaaaaaaaggaagagagggaaaaaat**gacaggcagaaggtcacgcctgg**ccctc
agtgcgctcctcaggcctctgctccagctggggctggcaggtggcggggggcaccagctcctccactccccacgccc
caccacagctttcaaagttaggaaacagggcaggt**GGAGGTGAAGTCCGAACAGA**

TTCACGCTTCACTTGTCTGCgtacctcattcttcttagacgcaggacaagagctctggcaaaggcgctgcagccacagagg
tttccggccggaaaaatcggcaccacagagatcccatgagaacgtcacgtacagcactgagacggagccctaataaaaact
gtggctct**gggtgataatgacgttactgtggg**ttcatcaactgtagcaaatc**gcctctgctggg**cggtgttgaaatgc
agaggctctggggggtcaggtatgtgggagctctctgtacctttcttgaatttgatgtgaacttaagctgctccaaaa
gataaaatcttgaagaaaagcgaaaaaaaaaaggaagagagggaaaaaat**gacaggcagaaggtcacgcctgg**ccctc
agtgcgctcctcaggcctctgctccagctggggctggcaggtggcggggggcaccagctcctccactccccacgccc
caccacagctttcaaagttaggaaacagggcaggt**GGAGGTGAAGTCCGAACAGA**

Deletions of the L1MC1-derived CTCF were confirmed via Sanger sequencing for two clones. The exact placement of the deletions is depicted in red.

Supplementary Figure 7: Virtual 4C Analysis of Downstream Enhancers

Virtual 4C Analysis of Downstream Enhancers



Virtual 4C analysis showing interactions between downstream enhancers and active domain in wildtype and L1MC1-KO lines.

Supplementary Table 1: Loop and TAD Call Data Sources

Data sources of loop and TAD calls used in all analyses.

Species	Structure	Assay	Cell Type	Link
Human	TADs	Hi-C	HSC_aml	https://www.biorxiv.org/content/10.1101/2020.04.18.047738v1
Human	TADs	Hi-C	HSC_aml	
Human	TADs	Hi-C	HSC_aml	
Human	TADs	Hi-C	HSC	
Human	TADs	Hi-C	HSC	
Human	TADs	Hi-C	HSC	
Human	Loops	Hi-C	HSC_aml	
Human	Loops	Hi-C	HSC_aml	
Human	Loops	Hi-C	HSC_aml	
Human	Loops	Hi-C	HSC	
Human	Loops	Hi-C	HSC	
Human	Loops	Hi-C	HSC	
Human	Loops	H3K4me2_ChIA-PET	CD4+ T Cells (CD4)	
Human	TADs	Hi-C	Cortex	https://www.nature.com/articles/nature11082
Human	TADs	Hi-C	hESC	
Human	TADs	Hi-C	IMR90	
Human	Loops	H3K27ac_HiC hIP	GM12878	https://www.nature.com/articles/ng.3963
Human	Loops	H3K27ac_HiC hIP	HCASMC	
Human	Loops	H3K27ac_HiC hIP	K562	
Human	Loops	H3K27ac_HiC hIP	MyLa	
Human	Loops	H3K27ac_HiC hIP	Naive_T	
Human	Loops	H3K27ac_HiC hIP	TH17	
Human	Loops	H3K27ac_HiC hIP	TReg	
Mouse	Loops	H3K27ac_HiC hIP	MES	
Human	Loops	CTCF_HiChIP	GM12878	
Mouse	Loops	CTCF_HiChIP	mESC	
Human	TADs	Hi-C	hESC	https://www.nature.com/articles/s41586-019-1812-0
Human	TADs	Hi-C	hESC	
Human	TADs	Hi-C	hESC	
Human	TADs	Hi-C	hESC	
Human	TADs	Hi-C	hESC	
Mouse	TADs	Hi-C	mESC	
Mouse	TADs	Hi-C	mESC	
Mouse	TADs	Hi-C	mESC	
Human	TADs	Hi-C	Lymphoma	

Human	TADs	Hi-C	Lymphoma		
Dog	TADs	Hi-C	Liver	https://www.ncbi.nlm.nih.gov/pmc/articles/PMC4542312/	
Human	TADs	Hi-C	RPE1	https://www.ncbi.nlm.nih.gov/pmc/articles/PMC4978254/#d36e641	
Human	TADs	Hi-C	RPE1		
Human	TADs	Hi-C	RPE1		
Mouse	TADs	Hi-C	PATSKI		
Mouse	TADs	Hi-C	mESC		
Rhesus Macaque	TADs	Hi-C	Fibroblasts		
Human	Loops	Hi-C	RPE1		
Human	Loops	Hi-C	RPE1		
Human	Loops	Hi-C	RPE1		
Mouse	Loops	Hi-C	PATSKI		
Rhesus Macaque	Loops	Hi-C	Fibroblasts		
Mouse	TADs	Hi-C	G1E-ER4		https://www.ncbi.nlm.nih.gov/pmc/articles/PMC5393350/
Mouse	TADs	Hi-C	G1E-ER4		
Human	TADs	Hi-C	Adrenal Cells (AD)	https://www.ncbi.nlm.nih.gov/pmc/articles/PMC5478386/	
Human	TADs	Hi-C	Aorta (AO)		
Human	TADs	Hi-C	Bladder (BL)		
Human	TADs	Hi-C	Cortex (CO)		
Human	TADs	Hi-C	GM12878		
Human	TADs	Hi-C	hESC (H1)		
Human	TADs	Hi-C	Hippocampus (HC)		
Human	TADs	Hi-C	IMR90		
Human	TADs	Hi-C	Lung (LG)		
Human	TADs	Hi-C	Liver(LI)		
Human	TADs	Hi-C	Left Ventricular (LV)		
Human	TADs	Hi-C	Mesendoderm (MES)		
Human	TADs	Hi-C	Mesenchymal (MSC)		
Human	TADs	Hi-C	NPC		
Human	TADs	Hi-C	Ovary (OV)		
Human	TADs	Hi-C	Pancreas (PA)		
Human	TADs	Hi-C	Psoas Muscle (PO)		
Human	TADs	Hi-C	Right Ventricular (RV)		

Human	TADs	Hi-C	Small Bowel (SB)		
Human	TADs	Hi-C	Spleen (SX)		
Human	TADs	Hi-C	Trophoblast-like (TRO)		
Human	Loops	Hi-C	THP-1_pma	https://www.ncbi.nlm.nih.gov/pmc/articles/PMC5610110/	
Human	Loops	Hi-C	THP-1		
Mouse	TADs	Hi-C	AML12	https://www.ncbi.nlm.nih.gov/pmc/articles/PMC5793783/ https://www.ncbi.nlm.nih.gov/pmc/articles/PMC6327227/	
Mouse	Loops	Hi-C	mESC		
Mouse	Loops	Hi-C	NSC		
Human	TADs	Hi-C	LCL	https://www.ncbi.nlm.nih.gov/pmc/articles/PMC6883528/	
Human	Loops	CTCF_ChIA-PET	Consensus		
Mouse	TADs	Hi-C	CH12-LX	https://www.ncbi.nlm.nih.gov/pubmed/25497547	
Human	TADs	Hi-C	GM12878		
Human	TADs	Hi-C	HeLa		
Human	TADs	Hi-C	HMEC		
Human	TADs	Hi-C	HUVEC		
Human	TADs	Hi-C	IMR90		
Human	TADs	Hi-C	K562		
Human	TADs	Hi-C	KBM7		
Human	TADs	Hi-C	NHEK		
Human	Loops	Hi-C	GM12878		
Human	Loops	Hi-C	HeLa		
Human	Loops	Hi-C	HMEC		
Human	Loops	Hi-C	HUVEC		
Human	Loops	Hi-C	IMR90		
Human	Loops	Hi-C	K562		
Human	Loops	Hi-C	KBM7		
Human	Loops	Hi-C	NHEK		
Mouse	Loops	Hi-C	CH12-LX		
Human	TADs	Hi-C	HAP1		https://www.pnas.org/content/112/47/E6456.long
Human	Loops	Hi-C	HAP1		
Human	Loops	Hi-C	HSC		https://www.sciencedirect.com/science/article/pii/S1097276520302604

Supplementary Table 2: L1MC1-KO1 HiC² Library Statistics

Sequenced Read Pairs	101,630,014
Normal Paired	90,448,638 (89.00%)
Chimeric Paired	4,407,936 (4.34%)
Chimeric Ambiguous	3,513,938 (3.46%)
Unmapped	3,259,502 (3.21%)
Ligation Motif Present	29,354,231 (28.88%)
Alignable (Normal+Chimeric Paired)	94,856,574 (93.34%)
Unique Reads	28,973,498 (28.51%)
PCR Duplicates	65,831,160 (64.78%)
Optical Duplicates	51,916 (0.05%)
Library Complexity Estimate	30,299,572
Intra-fragment Reads	325,061 (0.32% / 1.12%)
Below MAPQ Threshold	19,264,376 (18.96% / 66.49%)
Hi-C Contacts	9,384,061 (9.23% / 32.39%)
Ligation Motif Present	2,054,781 (2.02% / 7.09%)
3' Bias (Long Range)	69% - 31%
Pair Type %(L-I-O-R)	25% - 25% - 25% - 25%
Inter-chromosomal	2,431,679 (2.39% / 8.39%)
Intra-chromosomal	6,952,382 (6.84% / 24.00%)
Short Range (<20Kb)	2,615,029 (2.57% / 9.03%)
Long Range (>20Kb)	4,337,335 (4.27% / 14.97%)

Supplementary Table 3: L1MC1-KO47 HiC² Library Statistics

Sequenced Read Pairs	29,681,164
Normal Paired	26,419,325 (89.01%)
Chimeric Paired	1,505,030 (5.07%)
Chimeric Ambiguous	835,886 (2.82%)
Unmapped	920,923 (3.10%)
Ligation Motif Present	8,772,298 (29.56%)
Alignable (Normal+Chimeric Paired)	27,924,355 (94.08%)
Unique Reads	15,224,433 (51.29%)
PCR Duplicates	12,685,207 (42.74%)
Optical Duplicates	14,715 (0.05%)
Library Complexity Estimate	20,445,316
Intra-fragment Reads	166,830 (0.56% / 1.10%)
Below MAPQ Threshold	6,958,217 (23.44% / 45.70%)
Hi-C Contacts	8,099,386 (27.29% / 53.20%)
Ligation Motif Present	2,199,042 (7.41% / 14.44%)
3' Bias (Long Range)	71% - 29%
Pair Type %(L-I-O-R)	25% - 25% - 25% - 25%
Inter-chromosomal	1,929,082 (6.50% / 12.67%)
Intra-chromosomal	6,170,304 (20.79% / 40.53%)
Short Range (<20Kb)	2,227,463 (7.50% / 14.63%)
Long Range (>20Kb)	3,942,828 (13.28% / 25.90%)

Supplementary Table 4: GM12878 Wild Type HiC² Library Statistics

Normal Paired	269,686,068 (83.48%)
Chimeric Paired	16,914,983 (5.24%)
Chimeric Ambiguous	4,759,644 (1.47%)
Unmapped	31,677,013 (9.81%)
Ligation Motif Present	84,083,628 (26.03%)
Alignable (Normal+Chimeric Paired)	286,601,051 (88.72%)
Unique Reads	65,938,196 (20.41%)
PCR Duplicates	220,546,478 (68.27%)
Optical Duplicates	116,377 (0.04%)
Library Complexity Estimate	66,859,184
Intra-fragment Reads	799,217 (0.25% / 1.21%)
Below MAPQ Threshold	21,862,935 (6.77% / 33.16%)
Hi-C Contacts	43,276,044 (13.40% / 65.63%)
Ligation Motif Present	11,358,479 (3.52% / 17.23%)
3' Bias (Long Range)	71% - 29%
Pair Type %(L-I-O-R)	25% - 25% - 25% - 25%
Inter-chromosomal	7,210,469 (2.23% / 10.94%)
Intra-chromosomal	36,065,575 (11.16% / 54.70%)
Short Range (<20Kb)	15,110,002 (4.68% / 22.92%)
Long Range (>20Kb)	20,955,480 (6.49% / 31.78%)